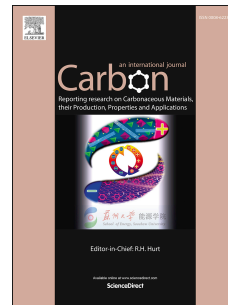


Accepted Manuscript

Scanning Curves of Water Adsorption on Graphitized Thermal Carbon Black and Ordered Mesoporous Carbon

Toshihide Horikawa, Takahiro Muguruma, D.D. Do, Ken-Ichiro Sotowa, J.Rafael Alcántara-Avila



PII: S0008-6223(15)30153-6

DOI: [10.1016/j.carbon.2015.08.034](https://doi.org/10.1016/j.carbon.2015.08.034)

Reference: CARBON 10199

To appear in: *Carbon*

Received Date: 8 June 2015

Revised Date: 11 August 2015

Accepted Date: 12 August 2015

Please cite this article as: T. Horikawa, T. Muguruma, D.D. Do, K.-I. Sotowa, J.R. Alcántara-Avila, Scanning Curves of Water Adsorption on Graphitized Thermal Carbon Black and Ordered Mesoporous Carbon, *Carbon* (2015), doi: 10.1016/j.carbon.2015.08.034.

This is a PDF file of an unedited manuscript that has been accepted for publication. As a service to our customers we are providing this early version of the manuscript. The manuscript will undergo copyediting, typesetting, and review of the resulting proof before it is published in its final form. Please note that during the production process errors may be discovered which could affect the content, and all legal disclaimers that apply to the journal pertain.

Scanning Curves of Water Adsorption on Graphitized Thermal Carbon Black and Ordered Mesoporous Carbon

Toshihide Horikawa^{1*}, Takahiro Muguruma¹, D. D. Do², Ken-Ichiro Sotowa¹, J. Rafael Alcántara-Avila¹

¹ Department of Advanced Materials, Institute of Technology and Science, The University of Tokushima, 2-1 Minamijosanjima, Tokushima 770-8506, Japan

² School of Chemical Engineering, The University of Queensland, St. Lucia, QLD 4072, Australia

*Corresponding author. E-mail: horikawa@tokushima-u.ac.jp (T. Horikawa)

Abstract

Adsorption isotherms of water on porous carbons generally show large hysteresis loops whose origin is believed to be different from simple gases adsorption in mesoporous solids. In this paper, we discussed in details the behavior of water adsorption isotherms and their descending scanning curves for two carbons of different topologies, a highly graphitized thermal carbon black, Carbopack F, and a highly ordered mesoporous carbon, Hex. For both solids, very large hysteresis loops are observed, but their behaviors are different. For Carbopack F, the loop extends over a very wide range of pressure and the loop is larger when the descending is started from a higher loading; while for Hex, the hysteresis loop shows distinct steps, the number of which depends on the loading where the descending starts. By carefully analyzing the scanning curves from different loadings, we established the mechanism of water adsorption in Hex as a sequence of three steps: (1) water molecules adsorb on functional groups located at the junctions between adjacent basal planes of graphene layers, (2) growth of water clusters around the functional groups, and (3) bridging of adjacent clusters to form larger clusters, followed by a complete filling of mesopores.

Keywords: Water adsorption; Scanning curve; Carbon black; Ordered mesoporous carbon

1. Introduction

Physical gases adsorption in porous materials has been considered as a promising technology for separation, for example, natural gas separation for energy supply [1] and carbon dioxide capture for environmental protection [2]. The adsorbents must meet a number of requirements: good affinity, selectivity, high capacity, good thermal and mechanical stability, good regeneration and acceptable cost. Porous carbon, such as activated carbon, molecular sieving carbon and carbon aerogel, is one of such classes of adsorbent [3], and most importantly this class of adsorbent can be tailored for the right pore size, volume and surface chemistry to suit specific applications. However, for it to perform well in separation, it must be able to deal with water as water always presents in most gaseous mixtures and it is very detrimental to the separation of desired substances because it competes for adsorption sites, resulting in a reduction in the efficiency of separation, especially when the humidity is greater than about 40% [4-7]. It is, therefore, very important to have a deeper understanding of how the porous structure and the surface chemistry affect the mechanism of water adsorption in porous carbon.

Water adsorption on activated carbon typically shows Type V, according to the IUPAC classification with a large H1 or H2 hysteresis loop [3, 8-11]. Hysteresis in water adsorption in non-porous and porous carbons is one of the least understood phenomena in adsorption, due to the complex interplay between the various interactions: (1) intermolecular interaction among water molecules, (2) interaction between water and the strong sites, for example functional groups where water can form very strong electrostatic interactions with, and (3) interaction between water and the graphene layers. The term “hydrophobic” interaction is commonly used to refer to the last interaction because it is the weakest interaction among the three interactions. It is, however, important to make it clear that the notion that water does not like graphene surfaces is not correct, but rather water molecules simply prefer to interact with themselves and functional groups on the surface. By increasing the temperature or by doping the graphene surface with either nitrogen or

oxygen (for example graphene oxide), water does indeed adsorb on the surface, rendering it “hydrophilic”. Many activated carbons can adsorb water in their micropores and mesopores because of the high concentrations of functional groups located either at the edges of the graphene layers or on the graphene layers, mainly at the defects [8, 12, 13]. It is now believed that the hysteresis observed in water adsorption in microporous carbons is not due to capillary condensation and evaporation, which is typically observed in adsorption of simple gases in mesoporous materials [14]. Adsorption of water in carbon was first put forward by Dubinin and co-workers [15], who proposed an entirely different mechanism than the capillary condensation and evaporation of simple gases in mesoporous media, where the Cohan/Kelvin equation applies [3]. Not only hysteresis of water adsorption is observed in porous carbons, but it also occurs with non-porous carbon, even with graphitized thermal carbon blacks (GTCB) [16]. We have reported water adsorption on Carbopack F (a highly GTCB) [16, 17] that the uptake is very small (almost insignificant) for pressures up to a relative pressure, P/P_0 , of 0.9, at which the uptake begins to increase steeply. Upon reducing P/P_0 from 0.99, the desorption branch does not trace the adsorption branch, resulting in a very broad hysteresis loop, spanning over the full range of pressure, with a lower closure point at a relative pressure of less than 0.001. To understand the origin of the broad hysteresis loop, we need to describe the mechanism of water adsorption in Carbopack F: at very low loadings, water molecules adsorb around the functional groups at the edges of the graphene layers because of the strong electrostatic interactions compared to the intermolecular interactions and the interactions between water and the graphene layer. As the loading is increased water clusters are formed around the functional groups and grow in size because of the greater electrostatic interaction between water molecules than the dispersive water-graphene interaction [17]. This mechanism of adsorption was taken into account in the recent theories for water adsorption in porous carbon [12, 18], and is also justified with molecular dynamics [19] and Monte Carlo simulations [20].

In this paper, we presented a detailed analysis of descending curves to shed even better light into the mechanisms of water adsorption and desorption from non-porous and porous carbons. Highly graphitized thermal carbon black, Carbopack F, and highly ordered mesoporous carbon, Hex, [21] are used to represent these two classes of carbon.

2. Experimental

2.1 Materials

A highly graphitized carbon black, Carbopack F (supplied by Supelco, USA) and a highly ordered mesoporous carbon [21], Hex, were used as the model adsorbents. Some of their properties relevant to this paper will be briefly given below and more details can be found elsewhere [16, 17, 21, 22]. Carbopack F consists of polyhedral micro particles (of the order of several hundred nm) with homogeneous graphene layers on the faces of the polyhedra, and nitrogen adsorption at 77K does not reveal any detectable pores [16, 17]. Hex has hexagon mesopores with a very sharp pore size distribution with a mean pore diameter of 9nm [22], the length of channel is longer than several hundred nanometer [21], and its pore surface is composed of graphene patches of 5nm in linear dimension [21]. Both carbon are graphitized at temperatures greater 2400K, resulting in a significant reduction in concentration of functional groups. By way of Boehm titration, the concentration is 0.07mmol/g in Carbopack F [16, 17, 23], which is grossly overestimated as concluded in our previous work [23]. In Table 1, the oxygen/carbon (O/C) ratio of samples is shown. The X-ray photoelectron spectroscopy (XPS) measurements were performed in a ULVAC PHI 5000 VersaProbe II spectrometer, with AlK α radiation (1486.6 eV) used for the excitation. All the binding energies were referenced to the C1s peak at 284.6 eV of C-C carbon. TEM images and the nitrogen isotherms of materials are shown in Supplemental data.

Table 1 Characteristic pore properties of Carbopack F [17] and Hex [21].

	S_{BET} [m ² /g]	V_{micro} [ml/g]	V_{meso} [ml/g]	O/C ratio
Carbopack F	4.9	0.00	0.00	0.0404
Hex	205 [22]	0.00	0.43	0.0498

S_{BET} = BET area obtained with nitrogen adsorption at 77K; V_{micro} = micropore volume; V_{meso} = mesopore volume obtained as nitrogen capacity at 0.98 and with an assumed liquid density.

2.2 Measurement

Water adsorption measurements were done at 298K using a high resolution volumetric adsorption apparatus (BELSORP-max, MicrotracBEL). The adsorption temperature was maintained with a water bath using an antifreeze coolant. To obtain each point on the isotherm, the system was first allowed to equilibrate for 300s and if the pressure change was less than $\pm 0.3\%$, the measurement was accepted as being at (quasi) equilibrium; if the change is larger than $\pm 0.3\%$, equilibration was continued for a further 300s until this criterion was met. Before each measurement of a new isotherm, the solid was degassed at 473K for 5h under vacuum (< 0.1 mPa) to remove any impurities. The descending scanning curves were measured from a predetermined pressure using the same apparatus.

2.3. Isostatic heat of adsorption

The isosteric heat was calculated by applying the Clausius-Clapeyron (CC) equation on isotherm data at two temperatures (formal derivation of CC equation can be found in Pan et al. [24]) close enough so that the derivative in the CC equation is replaced by the difference:

$$q_{iso} = -\Delta_{ads}H_{diff} = \frac{RT_1T_2}{T_2-T_1} \ln\left(\frac{P_2}{P_1}\right) \quad (1)$$

where R is the gas constant, T_1 and T_2 are the adsorption temperatures, and P_1 and P_2 are the respective absolute pressures at a given loading. In this study, we used isotherms at 283K and 298K to calculate the isosteric heats on Carbpacck F and Hex.

3. Results and Discussion

3.1 Water adsorption on Carbopack F and Hex

Water adsorption isotherms on Carbopack F and Hex at 298K are shown in Fig. 1.

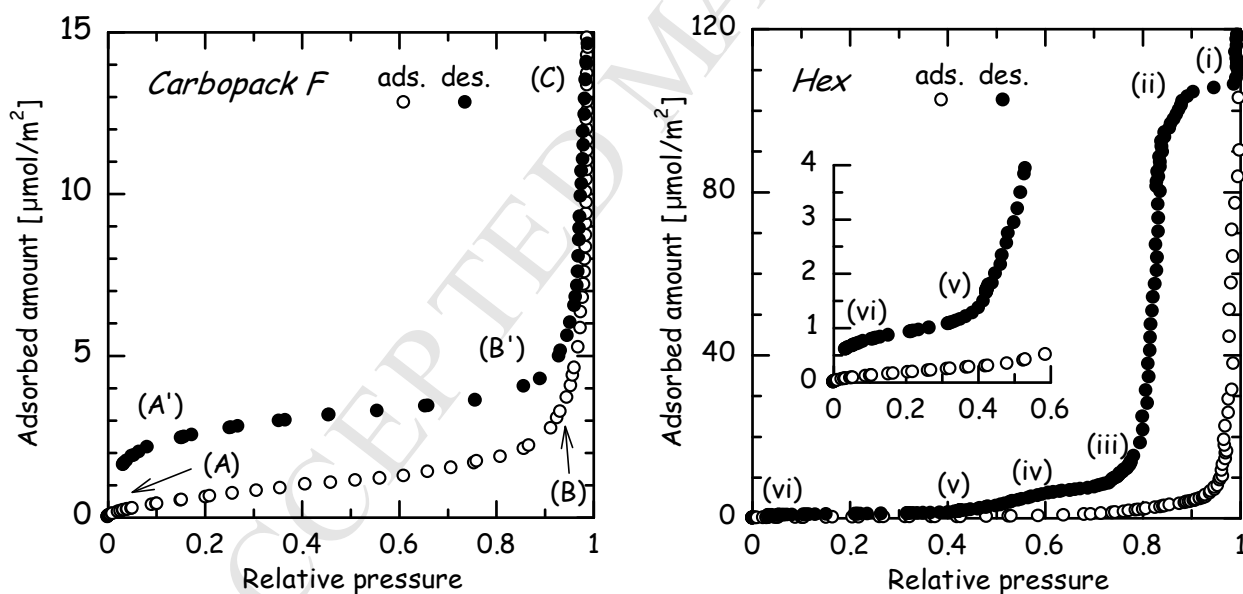


Fig. 1 Water adsorption and desorption isotherms on Carbopack F and Hex at 298K.

The water adsorption isotherms on Carbopack F have been discussed elsewhere [16], but we briefly describe here because they will form the basis for the subsequent discussion of descending curves in Carbopack F and Hex. The water adsorption amount increases slightly (almost insignificantly) for relative pressures up to 0.9, at which the uptake increases steeply (note the difference in the magnitude of the amount adsorbed in Carbopack F and that of Hex). The descending curve from a loading at a relative pressure of 0.99 (about $15\mu\text{mol}/\text{m}^2$) does not trace the adsorption branch, but rather forms a very large loop that spans over the full range of pressure. We could not determine the lower closure point because of the limitation of the instrument, but it is less than a relative pressure of 0.001. The hysteresis of water on the open surface of Carbopack F is due to cohesiveness of water clusters, brought about by the strong hydrogen bonding between water molecules and this interaction puts the clusters into a more meta-stable state with the progress of adsorption [14, 25]. As a result a much lower pressure is required to desorb water molecules from the functional groups. This is the reason why heating is required to facilitate the cleaning of the solid before the next measurement.

Mechanism of water adsorption on Carbopack F:

At low loadings, the uptake increases slightly with pressure, resulted from the nucleation of a complex between water and functional group, followed by the formation of water clusters which further grow within the interstices between the micro-crystallites, a process of which is distinctly different from the molecular layering of wetting fluids [26]. The effect of clustering can be quantified by considering the adsorptive capacity at a 0.9 relative pressure of $20\mu\text{mol}/\text{g}$ or $4\mu\text{mol}/\text{m}^2$, which is 5 times less than the amount that would hypothetically cover the graphite surface with a monolayer of water molecules [27]. Further experimental evidence was provided by Berezkina and Dubinin in 1969 with argon adsorption on a water-preloaded GTCB, and they showed convincingly that the argon adsorption isotherm is practically unaffected by the presence of pre-loaded water even when the water loading is equivalent to one hypothetical monolayer coverage

on the graphene surface [28]. Thus it is concluded that water adsorbs on the functional groups at the junctions between adjacent graphene layers and argon adsorbs on the layers, and this is supported with our recent simulation work [20].

Mechanism of water adsorption on Hex:

Water adsorption on mesoporous Hex was first reported by Morishige et al., using a gravimetric apparatus [29], and their isotherms are the same as ours obtained with a volumetric apparatus. Figure 2 shows the isotherms of Carbopack F and Hex for loadings less than $10\mu\text{mol}/\text{m}^2$ and we see that the adsorption in Hex up to 0.9 relative pressure is similar to that for Carbopack F, indicating that they follow the same mechanism in adsorption of nucleation of a complex, followed by clustering. The adsorption branch and the desorption boundary for Carbopack F at low loadings are approximately three times higher than those for Hex, indicating that the concentration of functional group in F per unit surface area is three times higher. By assuming the spacing between two adjacent functional groups in Hex is the same as that estimated for Carbopack F [23], we showed that the concentration of functional group in Hex per unit area is indeed three times lower than that of Carbopack F. We believe that this is a convincing proof that these carbons of different topologies share the same mechanism for water adsorption at low loadings.

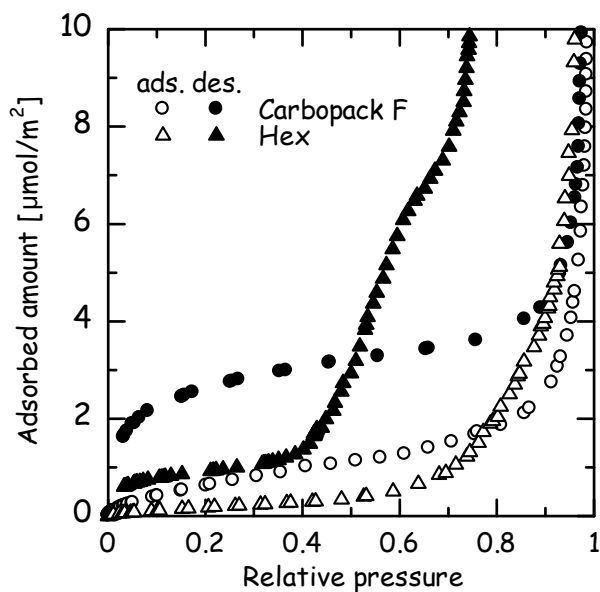


Fig. 2 Water adsorption and desorption isotherms on Carbopack F and Hex at 298K at low loadings.

Because of the steep rise in the adsorptive capacity beyond $P/P_0 = 0.9$, we did not detect any plateau for the saturation of mesopores with water. To determine this, we dosed the solid with very high water loading (greater than the amount that would be required to fill all mesopores) and then measured the desorption boundary. Interestingly the desorption boundary first traces the adsorption boundary reversibly at very high relative pressures close to unity, and this is attributed to the amount of water in the macropores (the interstices between the micro-particles or any large gaps in the system). Once these so-called occluded water molecules have been removed, the desorption boundary shows a plateau, signifying the onset of desorption of water from the mesopores. This plateau (about $100\mu\text{mol}/\text{m}^2$) represents the saturation mesopore capacity and it is extended to a reduced pressure of 0.8, at which the adsorptive capacity decreases very sharply to a capacity of about $20\mu\text{mol}/\text{m}^2$. This evaporation of $80\mu\text{mol}/\text{m}^2$ represents the capacity of water condensate in

the core of the mesopores. If the water in the mesopores is assumed to be bulk liquid like the volume occupied by water is estimated to 90% of that determined from nitrogen data, which is agreement with our previous work [12]. After a sharp decrease of the adsorptive capacity to around $20\mu\text{mol}/\text{m}^2$ the desorption boundary shows another gradual plateau to a loading of $6\mu\text{mol}/\text{m}^2$, followed by a greater decrease to a loading of $1\mu\text{mol}/\text{m}^2$, below which the behavior is similar to what we observed earlier with Carbopack F. These loadings of 100, 20, 6 and $1\mu\text{mol}/\text{m}^2$ must represent the different stages of desorption of water and hence their different states, and can't be attributed to different pore sizes in Hex [30] because it has a very narrow PSD with a mean pore diameter of 9nm [22]. Therefore, these different states of water during desorption can only be clarified with discussion of descending scanning curves at different loadings in Section 3.3.

3.2 Scanning curves of water adsorption on Carbopack F

The desorption scanning curves of water adsorption on the Carbopack F are shown in Fig. 3, with different starting loadings: 15, 8, 2, 1 and $0.5\mu\text{mol}/\text{m}^2$, corresponding to the relative pressures of 0.99, 0.98, 0.8, 0.4 and 0.1, respectively.

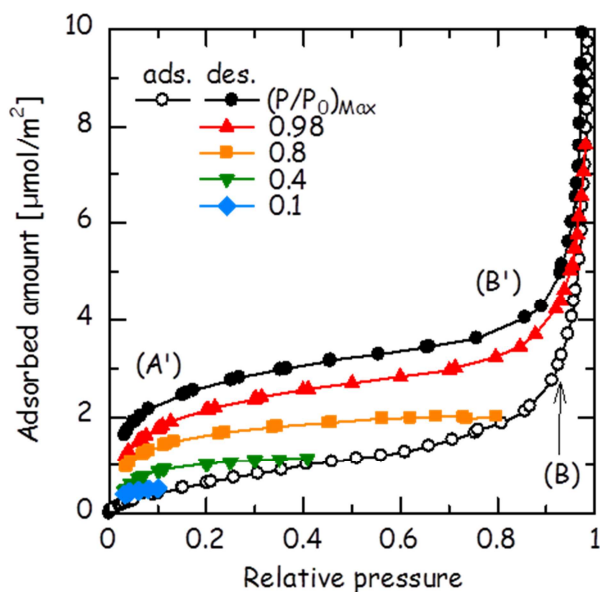


Fig. 3 Water desorption scanning curves on Carbopack F at 298K.

The scanning curves from loadings greater than $2\mu\text{mol}/\text{m}^2$ show the same pattern as the desorption boundary as shown in Figure 1, indicating a steep evaporation of occluded water followed by desorption of water molecules from the clusters. The scanning curve starting from the loading of $2\mu\text{mol}/\text{m}^2$ is very interesting because it is practically flat over a reasonably wide range of pressure, indicating that the clusters at this loading have a solid-like behavior, and we shall refer this loading as the critical loading. This means that for any loadings in excess of this critical loading water molecules are in a liquid-like state, in the form of liquid-like water around the clusters and the occluded water in the interstices between micro-crystallites. This is supported with the plot of the isosteric heat versus loading [17] where the isosteric heat reaches the heat of condensation at loadings greater than $2\mu\text{mol}/\text{m}^2$. The solid-like behavior of the clusters is also seen with “flat” descending scanning curves starting from loadings less than $2\mu\text{mol}/\text{m}^2$.

3.3 Scanning curves of water adsorption on Hex

The descending scanning curves for the Hex solid is shown in Figs. 4a and b, covering high and low loadings, respectively. The following observations are made:

- (1) Any descending scanning curves starting from loadings greater than $20\mu\text{mol}/\text{m}^2$ shows an initial crossing behavior to a relative pressure of 0.8, below which they show a similar pattern as the desorption boundary (black circle symbols). “Crossing” indicates the scanning curves across horizontally between adsorption branch and desorption branch of hysteresis of the desorption boundary.
- (2) When a descending scanning curve starts from any loadings between 20 and $6\mu\text{mol}/\text{m}^2$ we observed three distinct steps.
- (3) However, when the descending scanning curve starts from a loading between 2 and $6\mu\text{mol}/\text{m}^2$, the first step disappear.
- (4) Finally when it starts from a loading less than $2\mu\text{mol}/\text{m}^2$, we observed only one step, similar to what was observed with Carbo-pack F in Section 3.2.

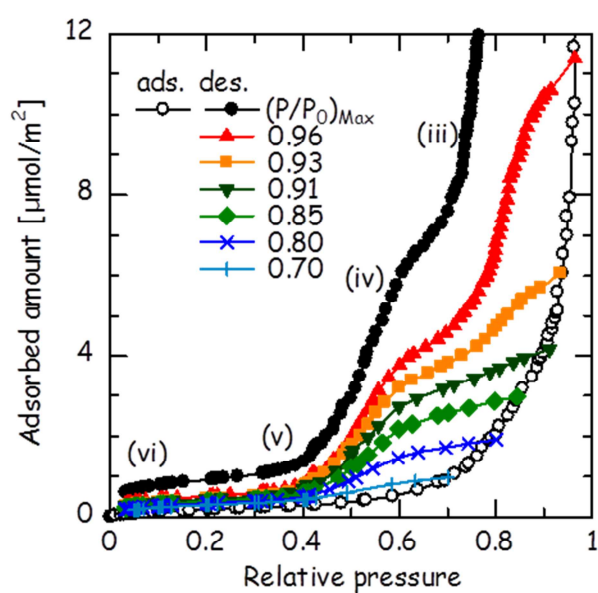
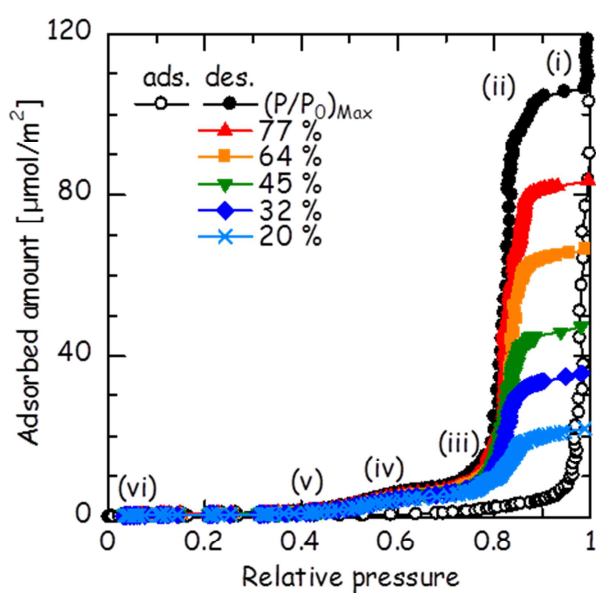


Fig. 4 Water desorption scanning curves on Hex at 298K. The percentages shown in the legends are the percentages of the adsorbed amount scaled against the total adsorbed amount, $107\mu\text{mol}/\text{m}^2$, in the desorption boundary (black circle symbols).

By comparing the scanning curves of the Hex and Carbopack F, we observed the step-like behavior for Hex, and this is due to the difference in the structure of the two solids: Carbopack F has very homogeneous basal planes of the surfaces of its polyhedron while Hex has hexagon pores whose graphitic walls are as homogeneous as surfaces of Carbopack F, but there are junctions between adjacent walls and they play an important role on how water adsorbs and desorbs, especially where the descending scanning starts.

During the course of the second step of scanning, we observed a sharp decrease in density in the relative pressure range between 0.4 and 0.6, a range that one would expect in most water adsorption isotherms for microporous carbons. Since there are no micropores in Hex and this sharp decrease must be due to the desorption of water molecules from single clusters around the functional groups.

To have a better insight on water molecules adsorbing in Hex, we plotted in Fig. 5a the water adsorption isotherm as the logarithm of the adsorbed amount versus the relative pressure, and its derivative along the adsorption branch.

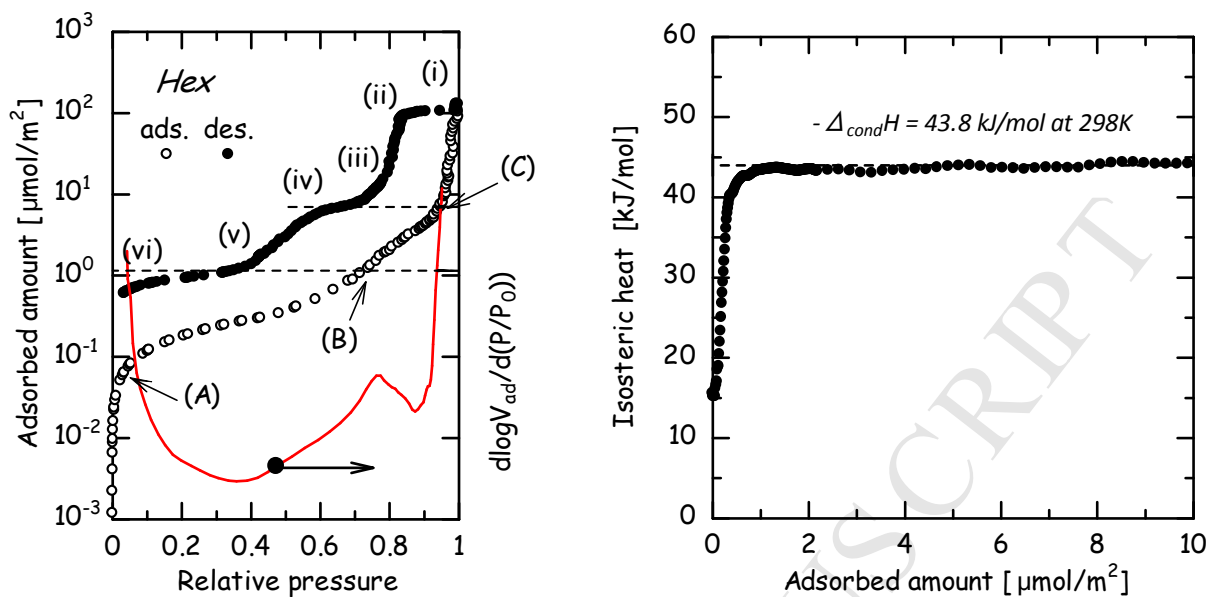


Fig. 5 (a) Water adsorption isotherm on Hex with the differential adsorbed amount of adsorption branch; (b) The isosteric heat of water adsorption on Hex.

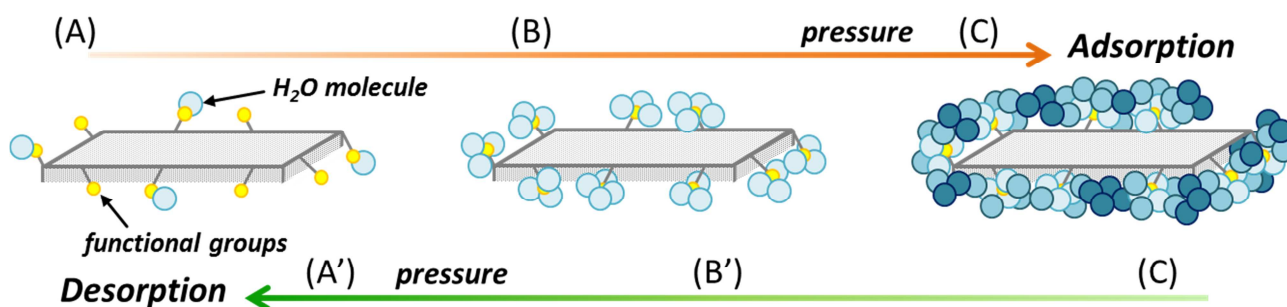
The adsorption branch exhibits three stages as the maxima in the derivative plot (solid line in Fig. 5a), and they also are manifested in the descending scanning curve from the filled pore (desorption boundary) shown as dashed lines. The second maximum corresponds to a loading of $1 \mu\text{mol}/\text{m}^2$, at which the isosteric heat approaches the heat of condensation (see Fig. 5b), indicating that water on the boundaries of the clusters in excess of this loading has liquid-like behavior. This occurs at a lower pressure than Carbpac F because of the stronger solid-fluid interactions brought about by the junctions in Hex solids. As the loading is further increased from 1 to about $10 \mu\text{mol}/\text{m}^2$ (between two dashed lines in Fig. 5a) clusters merge to form an adsorbed film covering the surfaces and this adsorbed film increases in thickness with its curvature approaching cylindrical, and finally water fills completely the mesopores of Hex.

At low loadings, the isosteric heat of water adsorption is around 15 kJ/mol which is associated with the nucleation of water around the functional groups [17]. The isosteric heat then increases with loading and approaches the heat of the condensation at loadings greater than $1\mu\text{mol}/\text{m}^2$, compared to $3\mu\text{mol}/\text{m}^2$ in the case of Carbopack F [17], indicating that clusters with liquid-like behavior are readily formed in Hex solid and this is evidenced with the lower heat at zero loadings for Hex.

3.4 Mechanism of water adsorption and desorption on Carbopack F and Hex

The schematics of the mechanisms of water adsorption and desorption on Carbopack F and Hex are shown in Fig. 6. The adsorption and desorption configurations at the same loadings are identical, except that they occur at different pressure, hence hysteresis.

Carbopack F



Hex

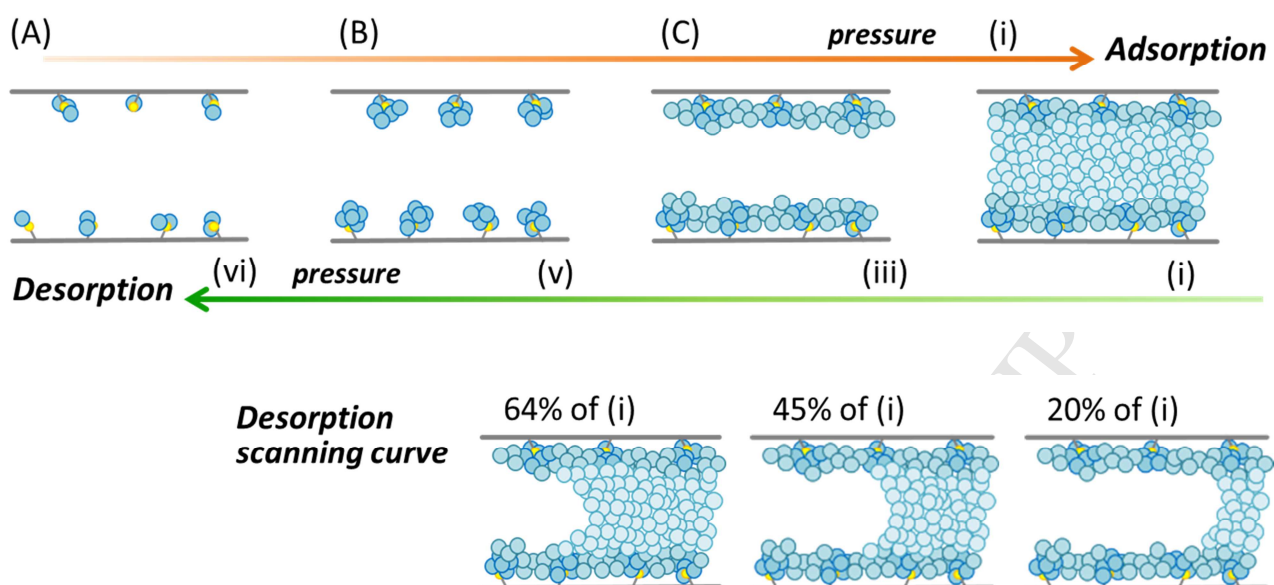


Fig. 6 The scheme of water adsorption and desorption on Carbopack F and Hex.

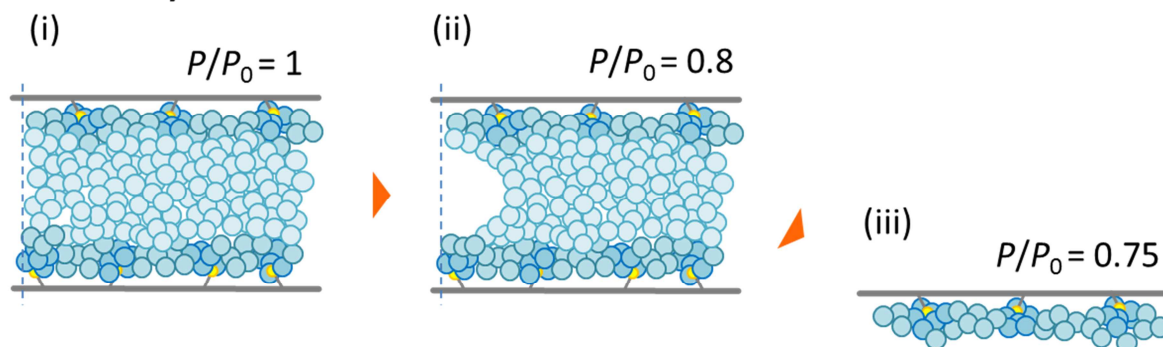
The hysteresis in the isotherm for Carbopack F is due to the increasing cohesiveness of the cluster formation from the configuration (A) to (B), brought about by the strong electrostatic interactions between water molecules and the functional groups.

For Hex, the mechanism from the configuration (A) to (B) is similar to that for Carbopack F, but it occurs over a lower pressure range because of the stronger solid-fluid interactions of the junctions in hexagonal pores. However, the mechanism from the configuration (B) to (C) in Hex is different from Carbopack F, in that the water clusters merge with their neighbors at P/P_0 of 0.75 to yield elongated clusters spanning along the junctions of the hexagonal pores. Further increase in pressure results in the spill over of water onto the pore walls, and an adsorbed film is then formed at a relative pressure of 0.95, above which capillary condensation occurs, filling the pore with water condensate by means of liquid bridges which increase their sizes with an increase in pressure.

The desorption of water from completely filled mesopores is very interesting as it reveals greater details about the states of adsorbed water. The configuration (i) in Fig. 6 is maintained until the

relative pressure reaches 0.8, at which the configuration (ii) shows a developed meniscus at the pore mouth (Fig. 7). A minute decrease of pressure from this point results in an evaporation of the condensate in the core of the mesopore to reach configuration (iii) where only the water adsorbed film remains on the pore walls. The desorption from the configuration (i) to (iii) of Fig. 6 is exactly the same as that observed with evaporation of simple gases from open ended pores. It is often suggested in the literature that the Dubinin theory could be applied for water adsorption in carbon, and this should be disputed in the light of the results obtained here. The descending scanning curves show a crossing behavior from the adsorption branch to desorption boundary when the adsorbed amount between 20 and $100\mu\text{mol}/\text{m}^2$, which is associated with the stretching of molecules of the liquid bridges filled partially of the pore, and when $P/P_0=0.8$ has been reached the water condensate in the core of the liquid bridge evaporates, resulting in a sharp drop in density to about $20\mu\text{mol}/\text{m}^2$.

Main desorption branch



Scanning curve

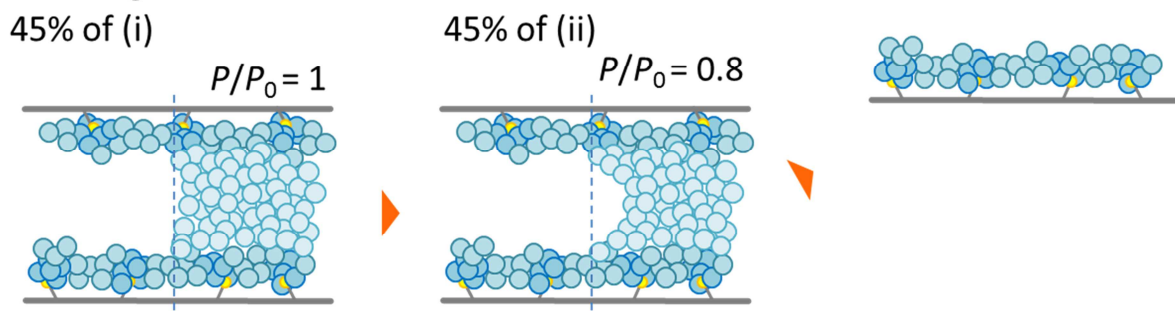


Fig. 7 The schematic mechanism of hysteresis on Hex at higher relative pressure.

After the condensate in the core of the liquid bridge has evaporated, hysteresis at loadings less than $10\mu\text{mol}/\text{m}^2$ (from the configuration (iii) to (v) in Fig. 4 or 5) must be to the removal of water molecules from the adsorbed film and subsequently from the clusters. The configuration (iii) represents the adsorbed film covering the pore surface, and this film is anchored to the surface via strong hydrogen bonding with discrete spatial distribution of the functional groups. This is the reason for the fragmentation of water condensate during the removal of water from the pore [29]. The energy required to remove a water molecule in the core of the liquid bridge is less than that to remove in the adsorbed film because of the stronger FF and SF interactions for water molecules in the film, and therefore the hysteresis in the second step is larger than the first step.

Further decreasing in pressure, the third step of the hysteresis is observed, and the energy required to remove water molecules in this step is the highest because of the combined effects of very strong fluid-functional group and fluid-fluid interactions. This is why the loop of the third step is widest and the lower closure point could not be achieved.

The hysteresis of the first step is associated with a capillary condensation mechanism, and therefore the following Kelvin equation can be used to estimate the pore size:

$$\ln\left(\frac{P}{P_0}\right) = \frac{-2\sigma V_m \cos\theta}{RT r_k} \quad (1)$$

where σ and V_m are the surface tension and the liquid molar volume of bulk water at temperature T , respectively, θ is the contact angle between liquid phase and pore wall, R is the gas constant, and r_k is the hydraulic radius of the core of the pore filled at the condensation pressure, P . With θ of $30\text{-}50^\circ$ [29] and the desorption relative pressure of the first step of 0.82, the Kelvin pore radius, r_k , is estimated as 4.6-3.4nm, respectively, which is in good agreement with the radius of 4.5nm

obtained from our comparison between our computer simulation and the experimental data [22]. Thus this is clear from the sharp evaporation of the first step is associated with the evaporation of the water condensate in the mesopore, also proving that water does fill the mesopore volume of Hex by the usual process of capillary condensation.

4. Conclusions

We have studied the water adsorption hysteresis on non-porous Carbopack F and on a highly ordered mesoporous carbon, Hex, which have hexagonal shaped pores. The hysteresis for Carbopack F spans over a wide range in relative pressure between 0 and 0.95. The descending scanning curves were measured in this study to shed greater insight into the mechanism of adsorption and the state of adsorbed water at different stages during desorption. Desorption is very sharp at high loadings and this is due to removal of occluded water in the interstices between crystallites, and at loadings lower than $2\mu\text{mol}/\text{m}^2$ the desorption is much more gradual (practically horizontal) because of the solid-like behavior of water in the clusters, rendering much wider loop in the low loading regions.

On the other hand, the hysteresis loop of water isotherm on Hex shows three steps: the first step occurs over the high pressure range and it is due to the desorption of the water condensate in the core of the mesopores. The second step is associated with the desorption of water molecules from the adsorbed film anchoring to the surface via discrete spatial distribution of functional groups. The third step of the hysteresis is the same as that for Carbopack F.

5. Acknowledgement

The authors thank to Prof. Morishige who supplied us the highly ordered mesoporous carbon. This work was partially supported by the Australian Research Council.

ACCEPTED MANUSCRIPT

References

- [1] Haruna K. Gas Separation by Pressure Swing Adsorption. *SHINKU*. 2000;43(12):1088-93.
- [2] Espinal L, Poster DL, Wong-Ng W, Allen AJ, Green ML. Measurement, Standards, and Data Needs for CO₂ Capture Materials: A Critical Review. *Environmental Science & Technology*. 2013;47(21):11960-75.
- [3] Rouquerol F, Rouquerol J, Sing KSW, Llewellyn P, Maurin G. Adsorption by Powders and Porous Solids, Second Edition: Principles, Methodology and Applications. London: Academic Press; 2013.
- [4] Wood GO. Affinity coefficients of the Polanyi/Dubinin adsorption isotherm equations: A review with compilations and correlations. *Carbon*. 2001;39(3):343-56.
- [5] Eissmann RN, LeVan MD. Coadsorption of organic compounds and water vapor on BPL activated carbon. 2. 1,1,2-Trichloro-1,2,2-trifluoroethane and dichloromethane. *Industrial & Engineering Chemistry Research*. 1993;32(11):2752-7.
- [6] Russell BP, LeVan MD. Coadsorption of Organic Compounds and Water Vapor on BPL Activated Carbon. 3. Ethane, Propane, and Mixing Rules. *Industrial & Engineering Chemistry Research*. 1997;36(6):2380-9.
- [7] Di Biase E, Sarkisov L. Molecular simulation of multi-component adsorption processes related to carbon capture in a high surface area, disordered activated carbon. *Carbon*. 2015;94:27-40.
- [8] Horikawa T, Kitakaze Y, Sekida T, Hayashi J, Katoh M. Characteristics and humidity control capacity of activated carbon from bamboo. *Bioresour Technol*. 2010;101(11):3964-9.
- [9] Thommes M, Morlay C, Ahmad R, Joly J. Assessing surface chemistry and pore structure of active carbons by a combination of physisorption (H₂, O, Ar, N₂, CO₂), XPS and TPD-MS. *Adsorption*. 2011;17(3):653-61.
- [10] Tóth A, László K. Chapter 5 - Water Adsorption by Carbons. Hydrophobicity and Hydrophilicity. In: Tascón JMD, ed. *Novel Carbon Adsorbents*. Oxford: Elsevier 2012, p. 147-71.

- [11] László K, Czakkel O, Dobos G, Lodewyckx P, Rochas C, Geissler E. Water vapour adsorption in highly porous carbons as seen by small and wide angle X-ray scattering. *Carbon*. 2010;48(4):1038-48.
- [12] Horikawa T, Sekida T, Hayashi Ji, Katoh M, Do DD. A new adsorption-desorption model for water adsorption in porous carbons. *Carbon*. 2011;49(2):416-24.
- [13] Miyawaki J, Kanda T, Kaneko K. Hysteresis-associated pressure-shift-induced water adsorption in carbon micropores. *Langmuir*. 2001;17(3):664-9.
- [14] Horikawa T, Do DD, Nicholson D. Capillary condensation of adsorbates in porous materials. *Advances in Colloid and Interface Science*. 2011;169(1):40-58.
- [15] Dubinin MM, Zaverina ED, Serpinsky VV. The sorption of water vapour by active carbon. *Journal of the Chemical Society (Resumed)*. 1955:1760-6.
- [16] Horikawa T, Takenouchi M, Do DD, Sotowa K-I, Alcántara-Avila JR, Nicholson D. Adsorption of Water and Methanol on Highly Graphitized Thermal Carbon Black and Activated Carbon Fibre. *Australian Journal of Chemistry*. 2015:-.
- [17] Horikawa T, Zeng Y, Do DD, Sotowa K-I, Alcántara Avila JR. On the isosteric heat of adsorption of non-polar and polar fluids on highly graphitized carbon black. *Journal of Colloid and Interface Science*. 2015;439(0):1-6.
- [18] Do DD, Junpirom S, Do HD. A new adsorption-desorption model for water adsorption in activated carbon. *Carbon*. 2009;47(6):1466-73.
- [19] Ohba T, Kaneko K. Kinetically Forbidden Transformations of Water Molecular Assemblies in Hydrophobic Micropores. *Langmuir*. 2011;27(12):7609-13.
- [20] Nguyen VT, Do DD, Nicholson D. A new molecular model for water adsorption on graphitized carbon black. *Carbon*. 2014;66:629-36.
- [21] Morishige K. Freezing and Melting of Kr in Hexagonally Shaped Pores of Turbostratic Carbon: Lack of Hysteresis between Freezing and Melting. *The Journal of Physical Chemistry C*. 2011:2720-6.
- [22] Wang Y, Nguyen PTM, Sakao N, Horikawa T, Do DD, Morishige K, et al. Characterization of a New Solid Having Graphitic Hexagonal Pores with a GCMC Technique. *The Journal of Physical Chemistry C*. 2011;115(27):13361-72.

- [23] Zeng Y, Prasetyo L, Nguyen VT, Horikawa T, Do DD, Nicholson D. Characterization of oxygen functional groups on carbon surfaces with water and methanol adsorption. *Carbon*. 2015;81(0):447-57.
- [24] Pan H, Ritter JA, Balbuena PB. Examination of the Approximations Used in Determining the Isothermic Heat of Adsorption from the Clausius–Clapeyron Equation. *Langmuir*. 1998;14(21):6323-7.
- [25] Thommes M. Physical adsorption characterization of nanoporous materials. *Chem Ing Tech*. 2010;82(Copyright (C) 2011 American Chemical Society (ACS). All Rights Reserved.):1059-73.
- [26] Cassel HM. Cluster Formation and Phase Transitions in the Adsorbed State. *The Journal of Physical Chemistry*. 1944;48(4):195-202.
- [27] Gregg SJ, Sing KSW. *Adsorption, surface area and porosity*. 2nd ed. ed. London: Academic Press; 1982.
- [28] Berezkina YF, Dubinin MM, Sarakhov AI. Adsorption of vapors on model nonporous adsorbents with a physically modified surface. IV. Low-temperature adsorption of argon vapors on graphitized carbon black with preadsorbed water or methanol. *Izv Akad Nauk SSSR, Ser Khim*. 1969(Copyright (C) 2015 American Chemical Society (ACS). All Rights Reserved.):2653-61.
- [29] Morishige K, Kawai T, Kittaka S. Capillary Condensation of Water in Mesoporous Carbon. *The Journal of Physical Chemistry C*. 2014;118(9):4664-9.
- [30] Klomkliang N, Do DD, Nicholson D. Hysteresis Loop and Scanning Curves for Argon Adsorbed in Mesopore Arrays Composed of Two Cavities and Three Necks. *The Journal of Physical Chemistry C*. 2015;119(17):9355-63.

Supplemental data

for

Scanning Curves of Water Adsorption on Graphitized Thermal Carbon Black and Ordered Mesoporous CarbonToshihide Horikawa^{1*}, Takahiro Muguruma¹, D. D. Do², Ken-Ichiro Sotowa¹, J. Rafael Alcántara-Avila¹¹ Department of Advanced Materials, Institute of Technology and Science, The University of Tokushima, 2-1 Minamijosanjima, Tokushima 770-8506, Japan² School of Chemical Engineering, The University of Queensland, St. Lucia, QLD 4072, Australia

*Corresponding author. E-mail: horikawa@tokushima-u.ac.jp (T. Horikawa)

Transmission electron microscopy (TEM)

Fig. S1 shows TEM image of Carbopack F [1, 2], and Hex [3]. Carbopack F has very homogeneous flat basal planes on the surfaces of the polyhedron crystallite, and Hex has hexagonal shape pores with graphitic walls.

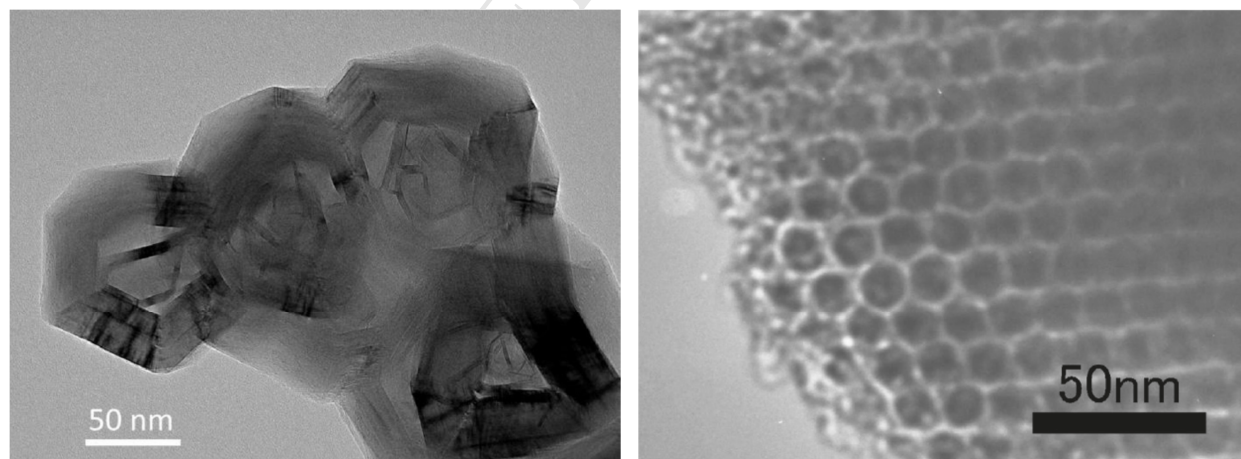


Fig. S1 TEM images of (left) Carbopack F [1, 2] and (right) Hex [3].

Nitrogen isotherms at 77K

Nitrogen isotherms of Carbopack F and Hex are shown in Fig. S2. Nitrogen isotherms were measured using a high resolution volumetric adsorption apparatus (BELSORP-max, MicrotracBEL). Before each measurement of a new isotherm, the solid was degassed at 473K for 5h under vacuum (< 0.1 mPa) to remove any impurities prior to any measurement.

N_2 isotherm on Carbopack F shows a typical shape of noble gas adsorption on a homogeneous flat surface with reversible adsorption and desorption branches. On the other hand, N_2 isotherm on Hex shows H1 type hysteresis, typically for solids having pores in the mesopore range.

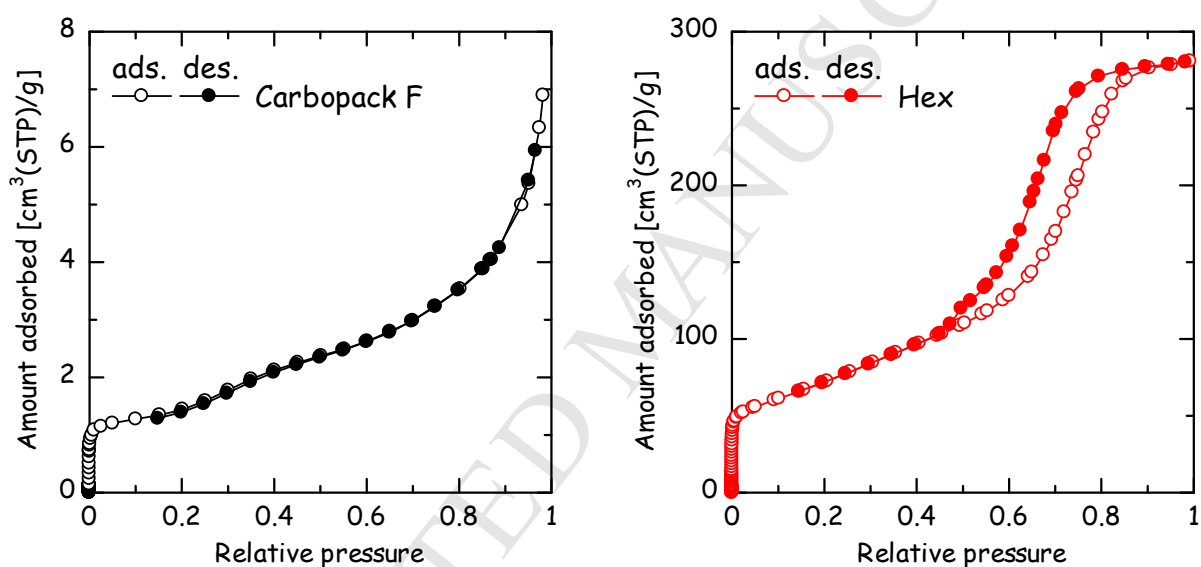


Fig. S2 Nitrogen isotherms of Carbopack F and Hex at 77K.

References

- [1] Horikawa T, Zeng Y, Do DD, Sotowa K-I, Alcántara Avila JR. On the isosteric heat of adsorption of non-polar and polar fluids on highly graphitized carbon black. *Journal of Colloid and Interface Science*. 2015;439(0):1-6.
- [2] Nguyen VT, Horikawa T, Do DD, Nicholson D. On the relative strength of adsorption of gases on carbon surfaces with functional groups: fluid–fluid, fluid–graphite and fluid–functional group interactions. *Carbon*. 2013;61:551-7.
- [3] Morishige K. Freezing and Melting of Kr in Hexagonally Shaped Pores of Turbostratic Carbon: Lack of Hysteresis between Freezing and Melting. *The Journal of Physical Chemistry C*. 2011:2720-6.